Acta Biol. Univ. Daugavp. 22 (1) 2022
ISSN 1407 - 8953

ASSESSMENT OF FOG INFLUENCE ON AUGMENTATION OF FLUORESCENT PARTICLES IN REAL-TIME BIOAEROSOL MEASUREMENT

Ingrida Šaulienė*, Lukas Vaitkevičius, Gintautas Daunys, Gediminas Valiulis, Laura Šukienė

Šaulienė I., Vatkevičius L., Daunys G., Valiulis G., Šukienė L. 2022. Assessment of fog influence on augmentation of fluorescent particles in real-time bioaerosol measurement. *Acta Biol. Univ. Daugavp., 22 (1): 1 – 18.*

Abstract
Bioaerosol is composed of biological origin particles dispersed in the air. They differ from airborne particles of non-biological origin in their ability to fluoresce. This biochemical property has been included into current detectors that operate in an autonomous mode and use laser-induced fluorescence to accurately identify biological particles. The challenging issue was observed on days with high air humidity and notably during fog. Monitoring data showed that during the fog, there are large numbers of fluorescent particles, potentially of biological origin, which occurrence is not explained. This study aimed to find out whether the raised number of fluorescent particles during fog impacts airborne pollen identification and describe the possible causes of the higher number of fluorescent particles during fog. Data from 2019 atmospheric observations were acquired with a fully automated Rapid-E detector in Lithuania for the study. The characteristics of each particle consisted of morphology data gathered using light scattering and data on biochemical properties collected using laser-induced fluorescence and fluorescence lifetime. The study concentrated on occasions in which extremely high numbers of fluorescent particles were detected in during fog. Our findings show that a large part of the fluorescent aerosol during fog is not pollen. The fluorescent traces of airborne particles refers that the fog creates specific conditions, and airborne particles identification may be compromised if scenarios are not integrated into bioaerosol particle recognition algorithms.

Keywords: bioaerosol, airborne pollen, laser-induced fluorescence, automatic airborne particles measurements

Corresponding author: Ingrida Šaulienė. Vilnius University, Šiauliai Academy, Vytauto Str. 84, Šiauliai, LT-76352, Lithuania, E-mail: ingrida.sauliene@sa.vu.lt*

Lukas Vaitkevičius, Gintautas Daunys, Gediminas Valiulis, Laura Šukienė. Vilnius University, Šiauliai Academy, Vytauto Str. 84, Šiauliai, LT-76352, Lithuania

INTRODUCTION

Aerosol plays an essential global role in the atmosphere; therefore, the behaviour of the environmental aerosol in the air is evaluated, and the parameters defining its physical and chemical state are studied (Valentini et al., 2020). The analysis of aerosol is performed for various purposes, for example, covering air quality aspects (EEA 2020, USEPA 2020) or investigating its indirect radiative effects on the climate system (Kazil et al. 2010). The interaction between water and aerosol in the atmosphere is complex and not fully explained. Scientific studies have proved the effect of aerosol on cloud genesis and existence (Shan et al. 2021), and the relation between the atmospheric aerosol formation and the involvement of aerosol particles themselves in cloud droplet activation has been established (Kerminen et al. 2005, Andreae & Rosenfeld 2008). The effect of aerosol particles on fog microphysics (Mazoyer et al. 2019) and the link between aerosol and droplet concentrations (Maalick et al. 2016) have been analysed. Primarily atmospheric aerosol is a complex mixture of suspended particles characterised by a considerable variation in chemical composition, size, and shape (Valentini et al. 2020). In studies, atmospheric aerosols analysing as primary organic aerosols (POAs) and secondary organic aerosols (SOAs). POA is an aerosol whose emission source can be both of anthropogenic origin, from industrial and combustion processes (Yan et al. 2019), and of natural origin (Schumacher et al. 2013). As pointed out by E. R. Lewisand S. E. Schwartz (2004), the largest source of naturally occurring POA is the ocean, but emissions from plants or soil are defined as a no less important resource (Fu et al. 2015; Williams & Després 2017). Particles emitted into the atmosphere by the biosphere are called primary biological aerosol particles (PBAP) (Frohlich-Nowoisky et al. 2016). In principle, SOA differs from the POA by its origin because SOA is formed in the atmosphere from reactive organic gases (Lim et al. 2005). Both POA and SOA could be analysed as a fluorescent aerosol group, provided that in both cases, we assess the fluorescent particles in the aerosol. The fluorescence characteristic of POA is caused by its constituent particles of biological origin, such as bacteria, pollen, spores or plant debris. Therefore, it is natural that POA is studied using fluorescence-based devices. On the other hand, Fu et al. (2015) argue that biogenic SOA derived from the photooxidation of isoprene and monoterpenes can also emit an intense fluorescence. In some cases, when identifying particles, the ability of SOA to fluoresce can be confusing, as fluorescent SOA may potentially be mistaken for biological particles by detection methods relying on fluorescence (Lee et al. 2013). In the physical and/or chemical sense, these are additional opportunities to investigate the secondary aerosol in more detail. However, the threat that the particles of biological origin may be confused with SOA is relevant. Recently, bioaerosol was increasingly observed in real-time using UV light-induced fluorescence-based devices (Crouzy et al. 2016; Chappuis et al., 2020). For analysing collected data and achieving the quality and accuracy of results, a new approach to the ability of aerosol to fluoresce is required. Currently, aerobiologists (studying airborne particles of biological origin) employ automatic particle detectors to perform research on bioaerosol and analyse the possibilities of this type of device to detect biological origin airborne particles in real-time. The technology that has become know-how in the aerobiology science allows researchers working in this field to obtain additional characteristics about fluorescence properties of airborne pollen or spores. In our previous bioaerosol studies (Daunys et al. 2021, Šaulienė et al. 2019a, Šaulienė et al. 2019b), we were aimed to identify airborne pollen from the overall composition of fluorescent particles.

Another aspect that is important for evaluating the accuracy of automatic particle detectors or their measurement capabilities is the state of the atmosphere at the time of measurement. Such atmospheric phenomena as fog can affect the measurement results. Fog is a complex phenomenon and plays an important role in atmospheric chemistry (Croft 2003). For example, compared with rain, fog contains higher levels of pollutants (Biswas et al., 2008). Studies have shown that fog can be a more important factor in the deposition of air pollutants than precipitation (Błaś et al. 2022). During fog, atmospheric properties change and processes taking place in the air can cause an increase in the number of fluorescent particles. Research has proved that fog water contains fluorophores. For example, J. E. Birdwell and K. T. Valsaraj (2010) investigated fog water and found that humic-like and biologically derived substances could represent fluorescent signatures representative of dissolved organic matter in fog water. On the other hand, fog increases the viability of biological processes of the so-called microbiological aerosol (Dueker et al. 2012). Researchers point out that fog droplets are a medium for bacteria, yeast and mould to form SOA (Fuzzi et al. 1997). It has been proved that fog droplets can be saturated with hydrophobic organic pollutants (Goss 1994), and SOA is more polar and hygroscopic than POA (Lim et al. 2005). It should be noted that mist episodes are not connected with aerosol activation (Zíková et al. 2020).

Aerosol has a relatively short residence time in the troposphere; therefore, it remains important to evaluate the regional signature of aerosol (Stocker et al. 2013) and to determine the role of fluorescent particles in the composition of atmospheric aerosol concerning the geographical area. The incidence of fog cases is also related to the geographical peculiarities of the area, and the results of studies performed in different countries show both a decrease (Avotniece et al. 2015) and an increase in fog cases (Hůnová et al. 2018). These arguments supplement and reinforce the need for a better understanding of the interaction between fog and fluorescent particles suspended in the atmosphere.

Real-time pollen observations revealed a significant increase in fluorescent particles recorded by a laser-induced fluorescence device during fog hours. The observational data leads to the presumption that additional information on the aerosol composition is recorded during the fog. The experimental results presented in this study aim to:

- find out whether the increased number of fluorescent particles during fog affects the identification of airborne pollen.
- describe the possible causes of the increase in fluorescent particles during fog.

Widening understanding provides valuable information on atmospheric aerosol and extends fog and bioaerosol studies using the data of laser-induced fluorescence. The new knowledge on fog fluorescence is an additional message for creating and developing algorithms recognising airborne pollen in real-time.

MATERIAL AND METHODS

Study area

Lithuania is located in the temperate climate zone and belongs to the southwestern subregion of the Atlantic continental forest area (LHMT 2020). The maximum annual air temperature in the eastern regions of the country usually occurs in late June and July (Galvonaitė et al. 2013). According to multi-annual monitoring data, the average air temperature in the warm period (April-October) was 12.7°C; and in the cold period (November-March) -1.2°C. Fog is a quite common phenomenon in Lithuania, as there are, on average, 23-95 days of fog per year, when the average duration of one fog is 4-6 hours (Galvonaitė et al. 2013).

The current study was performed on the data collected in Šiauliai. Šiauliai is the fourth largest city in Lithuania with about 100000 (OSP 2019) inhabitants. The observation site is in the central part of the city, about 200 m from the railway and within a radius of 500 m is surrounded by residential areas, supermarkets, and small squares. The nearest and largest park (~120 ha) with the vegetation typical of the geographical range is almost 2 km away. The state's air quality monitoring is carried out in Šiauliai permanently. The monitoring station is about 1.3 km from the observation site. According to air quality monitoring data, the concentration of PM10 does not exceed the limit value in the city. In 2019 there were 10 days when PM10 was above the norm and reached 51-93 μg/m^3 per day (EPA 2020).

Fog and mist data from meteorological station

This study is performed using fog data recorded in 2019 at the Šiauliai Meteorological Station of the Lithuanian Hydrometeorological Service. Information about fog is provided in two types of data. The first is in the form of phenomena recorded by an observer at the meteorological station, who assigns the code corresponding to the worldwide standards of WMO (WMO 2019) to the phenomenon. In this study, fog and mist events were analysed. For the analysis, we selected cases when mist (phenomenon code 10) due to change in meteorological elements or when mist (phenomenon code 4) that could have been formed due to the presence of smoke or dust in the air was identified. Fog is indicated by codes 41, 43, 45, 46 and 47, which depends on the course of fog development or prevalence of fog. Code 41 indicates fog in patches; 43 – the fog that became thinner during the preceding hour; 45 – the fog, but there is no appreciable change during the preceding hour; 46 – the fog that began or became thicker during the preceding hour (sky discernible); 47 – the fog that began or became thicker during the preceding hour (sky not discernible); 0 – means that no meteorological phenomena were detected.

The second data type is based on the meteorological visibility (expressed in meters) measured by the automatic weather station. The cases when the automatic weather station measured 20000 m of meteorological visibility are recognised as good visibility.

Bioaerosol measurement by automatic particle device

We collected data about ambient airborne particles between February 1 and October 31, 2019. For the study, an automatic Rapid-E particle device was installed at 20 m (55°55'35.9"N 23°18'31.2"E). The device aspirates ambient air with all its aerosol particles, and sample airflow is 2,8 litres per minute, with particles registered in the size range of 5-100 μm. The particle information includes data on morphological analysis based on the scattered light and chemical analysis based on laser-induced fluorescence and fluorescence lifetime. The last parameter was not used in this study according to the procedures described in Šaulienė et al. (2019b).

The Rapid-E indicates fluorescent particles in the total particle flow. Pollen was distinguished in the entire flow of air particles using our previously developed algorithm (Šaulienė et al. 2019b, Daunys et al. 2021). This study used the number of total particles (non-fluorescent and fluorescent) recorded by the device per minute and per hour and the hourly data of fluorescent particles, including total identified pollen. The associations between fog and fluorescent particles or pollen data were investigated by using the amounts of recorded particles per minute. The cases with exclusively large number of fluorescent particles when load reached ≥25000 fluorescent particles per hour, referred to as extreme cases.

Statistical evaluation of results

Data were statistically processed using R (R Core Team, 2018) and R Studio (R Studio Team, 2016). "GridExtra" (Auguie et al. 2017), "ggplot2" (Wickham 2016), and "gplots" (Warnes et al. 2016) packages were additionally used for the visualisation of the analysed results. The boxplot capabilities were employed to represent the continuous variables of total and fluorescent aerosol, expressed in the number of particles. The method allows evaluating the median of the number of particles recorded in 2019 and all outlying counts of particles individually. The upper and lower hinges corresponded to the first and third quartiles. Concentrated values of the collected data concerning the time scale were evaluated using a density plot. Kernel smoothing allowed us to get smoother distributions of variables, smoothing out the noise (data furthest from the mean) from the dataset. R-values and reliability values are given in the scatter diagrams between the total number of particles and fluorescent particles and the amount of pollen, noise data and total fluorescent aerosol. Typical days were selected to represent the signature of fluorescent particles, and graphs show the derived/calculated mean of fluorescence and scattering.

RESULTS

Quantitative analysis of bioaerosol

The aerosol recorded by the automatic particle device consisted of fluorescent and non-fluorescent particles (Fig. 1A). The fluorescent particles form about 21 % of the total particle volume, and the number of fluorescent particles is near directly proportional ($R = 0.7$, $p < 0.001$) to the scale of detected particles. The aerosol particles data density curve (extreme cases eliminated) highlights the routine load of the particles. Ordinarily, in the current study location, the number of fluorescent particles per hour was up to 10000. The median of fluorescent particles counts reached 1664, while of non-fluorescent particles, 6631.

Analysing the annual distribution of the ambient fluorescent aerosol (Fig. 1B), at the beginning of the year, the number of particles is higher and decreases during summer (June-August). The second peak is observed in autumn. Extreme values of fluorescent particles were recorded in March, August and October of 2019. The 9 extreme cases with more than 25000 fluorescent particles per hour were observed. In a total load of fluorescent particles, extremely high values are rare. Examination of air quality data (EPA 2020) on days when high levels of fluorescent particles were detected did not reveal any air pollution abnormalities.

We identified 84089 airborne pollen in a load of fluorescent particles detected by the automated particle device (Supplement Fig. 1). The highest numbers of pollen are calculated in spring and early summer. Assessing the daily distribution of fluorescent particles, the dynamics of pollen amount did not coincide with the general daily rhythm of fluorescent particles (Supplement Fig. 2). The maximum pollen values are identified between 9 am and 1 pm, UTC (Supplement Fig. 2A). The lowest content of pollen is recorded during the night and morning hours. The results are arranged differently according to the total number of fluorescent particles: the highest number occurs at 5-6 am (Supplement Fig. 2B).

Fluorescent particles and pollen identification during the fog events

Meteorological visibility is commonly used for synoptic purposes; our study associates visibility with the number of fluorescent particles and airborne pollen detected by an automatic particle detector. When analyzing the results of the number of fluorescent particles and pollen, we assessed whether meteorological visibility might have a direct effect on the number of detected particles.

No direct associations were found between meteorological visibility and particles indicated by the automatic device (Fig. 2). Analyzing the cases when the total number of indicated

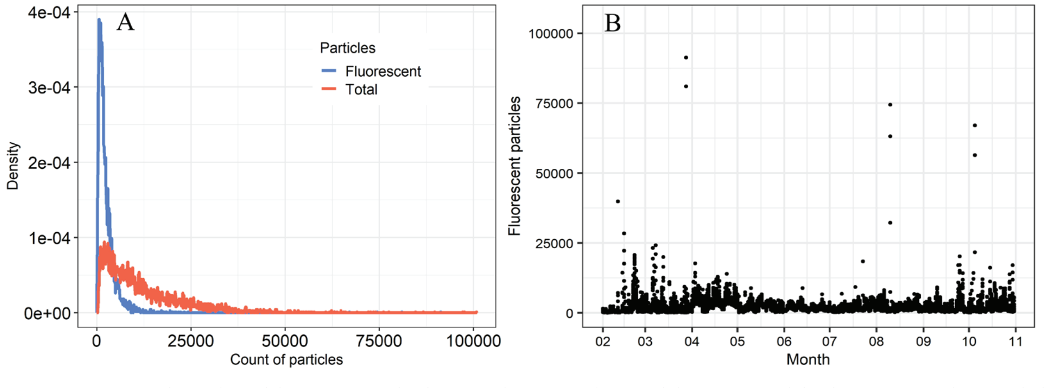

Figure 1. Results of ambient aerosol observations performed in 2019 with the automatic particle detector: A – the density curves of the number of recorded particles; B – scattering of fluorescent particles per hour in months.

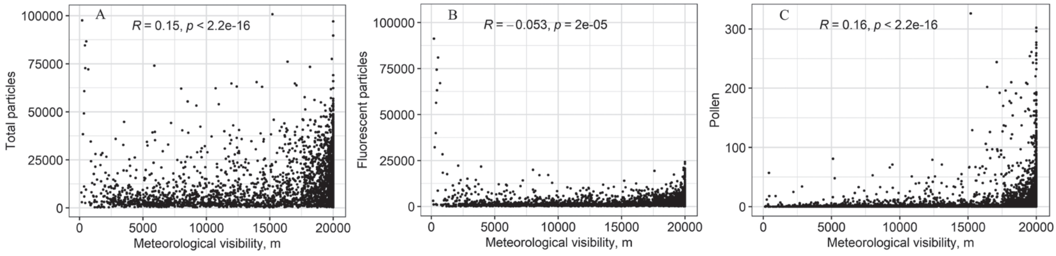

Figure 2. Distribution of aerosol particles with regard to atmospheric transparency: A – the diagram of the amount of total particles recorded by the automatic particle device and scattering of meteorological visibility; B – the distribution of fluorescent particles with regard to meteorological visibility; C - the distribution of identified pollen with regard to meteorological visibility.

particles reached more than 25,000 particles per hour, it is observed (Fig. 2A) that a high number of particles was recorded with good visibility (meteorological visibility - 20,000 m). A comparison of fluorescent particles and meteorological visibility (Fig. 2B) showed that an exclusively large number of fluorescent particles were not detected with good meteorological visibility. Conversely, when the visibility registered at the meteorological station was low and prevailed in the range of 200-692 meters, an exceptionally high number of airborne fluorescent particles was detected. In these conditions, the average number of fluorescent particles per hour was 26161; meanwhile, with the increase of meteorological visibility from 1000 m to 5000 m, the average number of fluorescent particles was only 6284.

Based on the information collected by the automatic particle detector, the pollen recognition algorithm allows the identification of pollen (Fig. 2C) in the fluorescent aerosol. During the hours when an extremely high number of fluorescent particles is registered, pollen is not detected among these particles or a small amount of pollen is identified (Fig. 3B, 3C). In these cases, we detected 89 pollen. We analyzed whether there is a relationship between meteorological visibility and the amount of pollen identified in the flow of fluorescent particles. The data recorded by the automatic detector in real-time demonstrate that the amount of pollen in the air is the highest when meteorological visibility is 20000 m. When assessing the links between pollen content and meteorological visibility, it is observed that the better the visibility, the higher amount of airborne pollen ($R=0.16$, $p<0.05$). After evaluating the relationships between meteorological visibility and the number of fluorescent particles and concluding that the extreme cases were associated with a significant decrease in visibility (Fig. 2B), the extreme cases were compared with the phenomenon of fog recorded at the meteorological station (Fig. 3). Exceptionally high levels of fluorescent particles (> 25,000 per hour) were detected 9 times during the study period. There was one case each on February 11 and February 15 at 2 p.m., when the number of fluorescent particles reached 39873 and 28386 particles per hour, respectively. On March 28 and October 5 (Fig. 3), were found two cases both at 5 and 6 a.m. in the morning. On March 28, the number of particles was 91269 and 81029, and on October 5 - 56380 and 67076, respectively. On August 10, three such cases were identified: 3 a.m. - 74422, 4 a.m. - 63179 and 5 a.m. - 32194. Total for 2019 during the study period was five days, with an extremely high number of fluorescent particles. On February 11 at 2 p.m. and February 15 at 9 p.m., the fog was not recorded at the meteorological station, but the meteorological visibility during extreme events was 348 m and 877 m, respectively. Rain showers (slight) and drizzles (not freezing, continuous) were recorded at the weather station during these hours.

Fog cases were recorded 3 of 5 days at the meteorological station. The 3-day fog recording

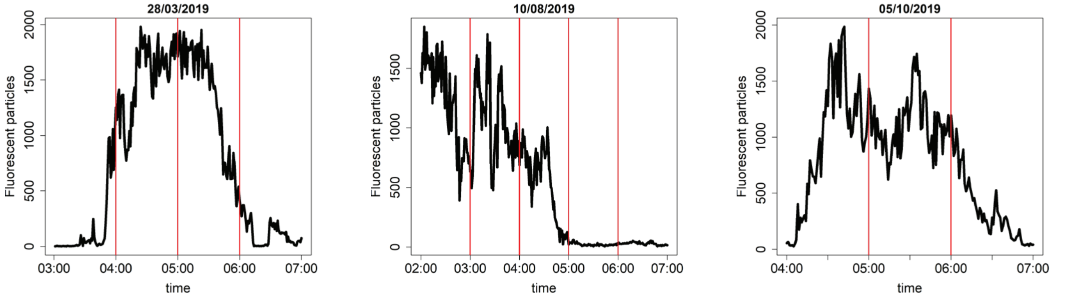

Figure 3. Numbers of particles making up fluorescent aerosol and fog cases, when fluorescence particles > 25 000 per hour. The red line marks hours during which fog cases were recorded at the meteorological station (code: 41-47).

cases and the fluorescent particle numbers per minute are shown in Fig. 3, following the principle that the dynamics of the fluorescent particle should be shown one hour before and one hour after fog recording. This method was chosen because the fog data recorded at the meteorological station were instantaneous.

Fig. 3 showed that when a considerable number of fluorescent particles were detected, 9 cases of fog were recorded on these days. The number of cases of fog per day differs, i.e., from two to four cases were identified. The results revealed that the occurrence of extreme events might be associated with the phenomenon of fog. Meteorological visibility data support this assumption. In the hours when the extreme cases were detected, the visibility was 200-692 m. On the other hand, during the study period (February-October) in 2019, 16 cases of fog were recorded over eight days. Consequently, there were cases when the fog was recorded at the meteorological station, but the number of fluorescent particles did not exceed the average values determined in the particular year. The dynamics of cases are displayed in Supplement Fig. 3. In those cases when the fog was not detected either visually or at the automatic meteorological station, the particle detector recorded an average of about 40 fluorescent particles per minute. The graphs show no uniform trend regarding the effect of fog on the number of particles. According to the automatic detector measurement readings under the conditions of fog in patches, the number of particles in the atmosphere is close to the values recorded in good meteorological visibility.

A more detailed analysis linking the number of fluorescent particles and the amount of airborne pollen with the atmospheric phenomena revealed the influence of mist on particle number and showed associations with similar atmospheric phenomena such as mist. Change in the amount of pollen and fluorescent particles depending on meteorological phenomena related to fog and mist is displayed in Fig. 4. Those days when no phenomena related to precipitation or fog are recorded (code 0) are more favourable for pollen dispersal (Fig. 4 A). It should be noted that small amounts of pollen are detected in fluorescent aerosol during fog (on average 8 pollen per hour), but during those hours, the fluorescent particles in the air are particularly abundant (on average 31445 particles per hour). Pollen is detected during both fog and mist. When distinguishing the maximum values for pollen content, it should be noted that during fog, 57 pollen per hour were identified, while during mist, 81. Assessing the cases when the mist is identified both due to meteorological conditions (code 10) and increased dustiness (code 4), it can be envisaged that the amounts of fluorescent particles are lower than in fog.

The highest amounts of fluorescent particles were registered in the presence of different types of fog phenomena (Fig. 4B). More frequent cases (4 out of 7) where fluorescent particles

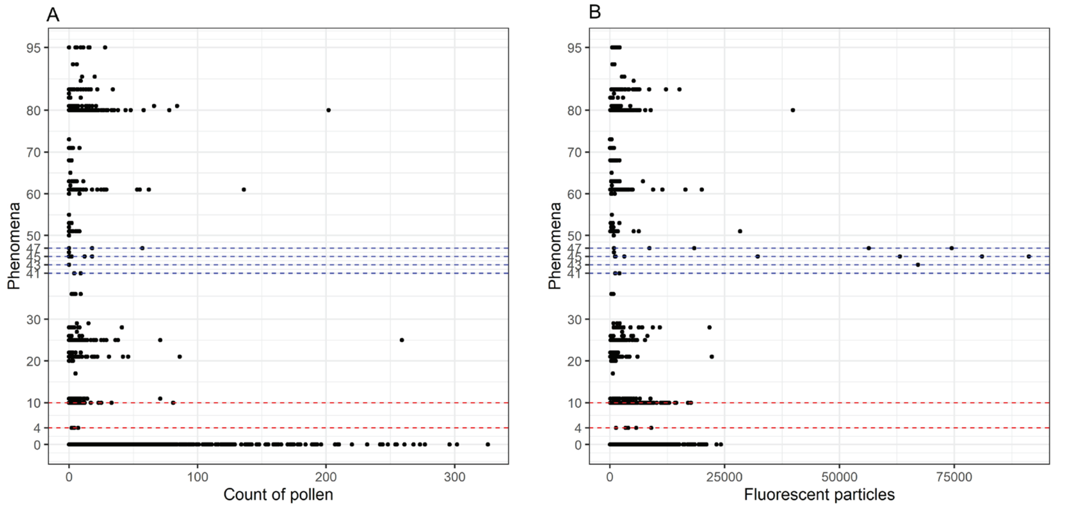

Figure 4. Distribution of pollen detected in fixed aerosol (A) and of fluorescent aerosol particles (B) with regard to atmospheric phenomena (blue – fog-related phenomena; red – mist-related phenomena).

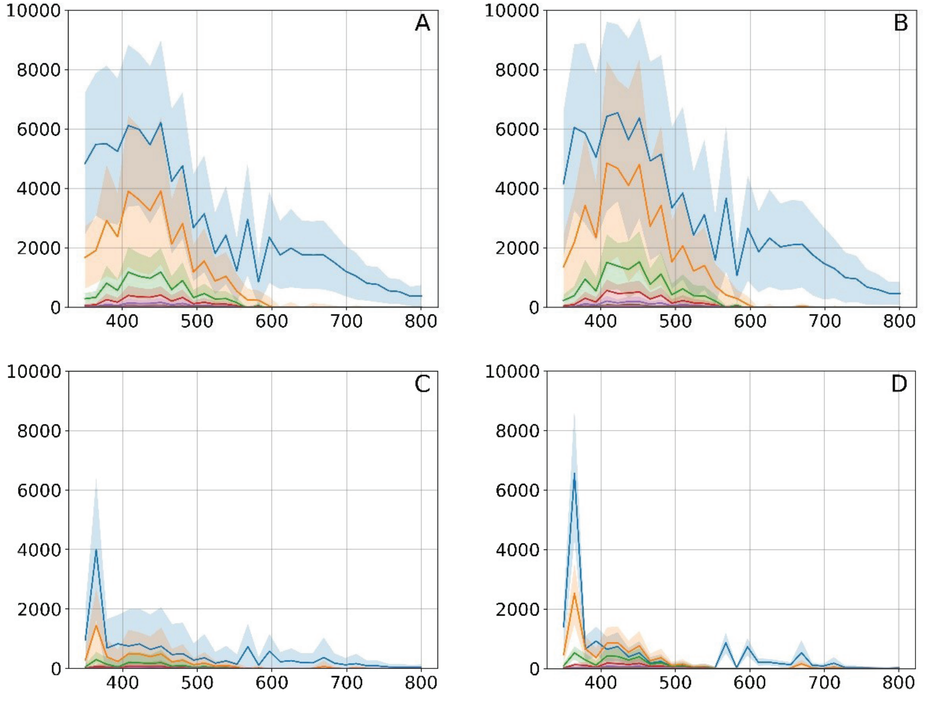

Figure 5. Average fluorescence signature of detected airborne particles: A – pollen when no atmospheric phenomena are identified and meteorological visibility reaches 20000 m (relative humidity <40%); B – pollen during fog; C – particles when no atmospheric phenomena are identified and meteorological visibility reaches 20000 m (relative humidity <30%); D – particles during fog. The blue line indicates the signal of the first fluorescence lifetime moment, and all other lines are delayed by following the 500ns step from the last fluorescence lifetime moment signal. Shadows indicate standard deviation. The x-axis denotes the wavelength in nm; the y-axis, the amplitude delayed (no units).

increase significantly in the presence of fog, but there is no appreciable change during the previous hour (45). In the case of fog in patches (41), the amounts of fluorescent particles are small. Summarizing the results described above, and Fig. 4B, during fog, the automatic particle detector detects significantly higher amounts of particles than on days without phenomena or in cases of other types of meteorological phenomena.

Fluorescent signature of airborne particles

The data recorded by the automatic particle detector were analysed employing the algorithm designed and developed for this device (Šaulienė et al., 2019b). Typical examples of images of particles identified by it are presented in Fig. 5.

The pollen signature (Fig. 5A and 5B) is similar both in hours without atmospheric phenomena and in the fog environment. Seeking the accuracy of the result, we selected data for representation, which are recorded during a typically expressed atmospheric phenomenon. The mismatches between amplitudes, seen in the figure, are related to differences in pollen determined by the plant species. The signature of pollen significantly differs from that of other fluorescent particles (Fig. 5C and 5D). The image of other (non-pollen) fluorescent particles, composed based on average amplitude and wavelength data, is similar irrespective of whether fog had formed or not. It should be noted that the peaks of the signal of the first lifetime moment (Fig. 5A and 5B) are at the same wavelength (365 nm). The similarity is observed at the wavelengths of 568 and 597 nm when two repetitive peaks are identified. Based on the peculiarities of signal suppression, it can be seen that in fog cases, the signal of the second lifetime moment manifests itself atypically. We noticed such a trend when analysing fog cases (the figure for each case is presented in supplements) when the number of fluorescent particles exceeds 50000. This reveals the need to evaluate the behaviour of the particle fluorescence signal and to eliminate such cases by algorithms while forming pollen identification algorithms.

DISCUSSION

Airborne particle fluorescence is an important property of particles, enabling the characterisation of the composition of atmospheric aerosol and other peculiarities (Pöhlker et al. 2013). In this study, we provided an exhaustive analysis of the increase in fluorescent particles, which shows up when air composition is registered with a Rapid-E automatic detector (Fig. 2). The use of automatic detectors collecting airborne particles data for scientific or even monitoring purposes is growing (Oteros et al. 2015; Clot et al. 2020, Šaulienė et al. 2019b, Mainelis 2020), while knowledge about the composition of atmospheric particles is insufficient (Fröhlich-Nowoisky et al. 2016, Šantl-Temkiv et al. 2020, Kabir et al. 2020).

Bioaerosol particles are considerably different in size, type, biological properties or geographical distribution, making their detection and identification in real-time more complex than gaseous or particulate matter. The role of the latter concerning atmospheric composition has been studied quite comprehensively, and the available knowledge and experience are used for air quality assessment (EEA 2020, Hyde & Mahalov 2020, USEPA 2020). The source of bioaerosol in nature can be soil, water, animals, and plants (Fu et al. 2015, Heath et al. 2017); therefore, it contains various types of organic biological material (Jaenicke 2005, Grewling et al. 2019) that forms primary biological aerosol particles (PBAP) (Després et al. 2012, Shiraiwa et al. 2017). The property of PABP – the intrinsic fluorescence occurring due to the presence of biological fluorophores (coenzymes, biopolymers, chlorophyll) everywhere in the cells is used to distinguish the biological origin particles from other particles. The analysis of data collected with an ultraviolet light-induced fluorescence (LIF) detector in 2019 has shown that, the recorded number of fluorescent particles is commonly less than of non-fluorescent ones (Fig. 1). The trend would probably not be new and worth discussing if not for the exceptional abundance of fluorescent particles identified during observations, which consistently coincides with the cases of low meteorological visibility (Fig. 2). The identification of fluorescent particles is important both from a biological perspective and the perspective of human health protection (Biswas et al. 2008, Pöhlker et al. 2013, Grewling et al. 2019, Donaldson, 2020). Depending on the peculiarities of aerosol and meteorological conditions, the lifetimes of particle residence in the atmosphere can vary from a few hours to several weeks (Fröhlich-Nowoisky et al. 2016). In developing the implementation of the idea of characterising bioaerosol composition in real-time into daily monitoring practice, it is necessary to find out the reasons causing the significant increase in the number of fluorescent particles in the air. One thing that is clear from the evaluation of available results is that the number of fluorescent particles significantly increased during the hours when the fog was recorded (Fig. 3). Besides, the thicker the fog, the more fluorescent particles are in the air. The peculiarities of the particles formed during fog are usually studied in the collected fog water rather than using direct measurements. It has been found that dissolved organic matter in fog water consists of humic-and-protein-like fluorophores commonly found in macro and microorganisms in terrestrial samples (Birdwell & Valsaraj 2010). Examination of fog water by microbiological methods has shown that water is rich in bacteria and microscopic fungi, which act as culture media for viable particles (Fuzzi et al. 1997). Researchers who have studied the microbiological environment of water relate their results to the probability that the identified microorganisms could represent an atmospheric source of SOA. In atmospheric oxidation processes, biogenic substances such as isoprene or monoterpenes induce fluorescence of biogenic SOA (Lee et al. 2013). In addition, after heavier dew or fog, pollen releases large amounts of allergenic particles (Taylor et al. 2004, Rathnayake et al. 2017), which can increase the number of fluorescent particles in the air as well.

Pollen from anemophilous plants change the composition of bioaerosol in a particular territory during the vegetation period (Williams & Després 2017). At the same time, there is considerable evidence of long-distance transport of pollen (Siljamo et al. 2008, Sofiev et al. 2013, Myszkowska et al. 2021), which confirms that the number of airborne particles registered by automatic devices could increase due to long-distance transport. Our results have demonstrated that pollen detected by the automatic detector in 2019 formed a small share of fluorescent particles, especially during fog. The results are in line with the prevailing theory that atmospheric humidity affects the concentration of pollen in the air, and the latter significantly decreases when relative humidity increases or fog is recorded (Pérez et al. 2009). The automatic detector used in this study detected most pollen in good meteorological visibility, although there are studies that have demonstrated that light rain does not reduce pollen concentrations in the air (Kluska et al. 2020).

The average daily distribution of fluorescent particles, i.e., that have been assigned not to pollen by the algorithm can be associated with different factors. The fact that the number of fluorescent particles is higher in the morning hours can be related both to the change in daily humidity in the air and to the emission caused by anthropogenic activities in the urban area. The assumption about the human influence on the growth of fluorescent particles can also be made because of the observed increase of particles in the afternoon hours. Substantiation of these assumptions requires comprehensive research. Their results would not only help to better understand the manifestation of the dynamics of fluorescent particles but would also be useful in modelling aerosol dispersion in urban areas.

Real-time automatic particle detectors are used to distinguish allergenic pollen from bioaerosol, which is particularly important for public health care and prevention. Our results show that identify pollen recorded during fog from the total fluorescent flow is possible due to the typical characteristic of fluorescence. The obtained results also confirm that during fog, particles of biological origin can be identified in a fluorescent aerosol detected by real-time automatic particle detectors. Lee et al. (2013) state that fluorescent SOA can hinder the recognition of biological particles. Our results highlighted the pollen fluorescence signature enabling the algorithm to recognize pollen from other fluorescent particles in POA or SOA. Pöhlker et al. (2013) argued that the autofluorescence of pollen was intrinsically different from bacteria and fungal spores, based on the fact that it did not originate from proteins and other cytosolic compounds but rather from cell wall associated fluorophores. Sporopollenin present in the pollen wall sexine (Blackmore et al. 2007) is an extremely chemically inert biopolymer found in pollen and spores of terrestrial plants (Li et al. 2019). According to other authors (Donaldson 2020, Roshchina et al. 2002), not only sporopollenin but also flavonoids or pigments (carotenoids, lipofuscin) can fluoresce in the pollen wall. Pollen is characterized by three fluorescence peaks: 475, 565, and 675 nm (Urbanczyk et al. 2015). These peaks are likely related to sporopollenin (blue fluorescence) and flavonoids or pigments (green/yellow fluorescence) (Donaldson 2020). Our results show that the maximum amplitudes of the first signal of the pollen fluorescence signature are in the spectral range from 365 nm to 481 nm, while the peak of the amplitude of the particles that are not assigned to pollen is only at 365 nm. At the wavelengths of 568 and 597 nm, two repetitive peaks were detected concerning both pollen and fluorescent particles that have not been assigned to them. The information recorded by the automatic particle detector, reflecting fluorescence peculiarities, is possibly related to sporopollenin and flavonoids or pigments in pollen. It is also noteworthy that fog has not substantially altered pollen fluorescence signatures recorded by the particle detector. In the case of other particles that fluoresced during fog, which were not classified as pollen by the algorithm, different amplitudes of fluorescence were recorded compared with cases when the fog was not registered.

In the future, focusing on fluorescence-based devices, fog-induced particle content in the algorithms for recognition of detected particles must be evaluated. On the other hand, there is a lack of more detailed knowledge about the origin of fluorescent particles recorded by real-time automatic particle detectors, highlighting the complex composition of bioaerosol with regard to the geographical area.

CONCLUSIONS

1. Fluorescence is a specific property of biological origin particle and knowledge of the mechanism of fluorescence allows it to be used to identify particles in the air. For the analysis of bioaerosol using automatic detectors, it is important to pay attention not only to the fluorescence of the particles, but also to the processes occurring in the atmosphere during which the composition of aerosol may change or decrease detection capabilities in devices.

2. The study results show that the number of fluorescent particles with a size of 5-100 μm registered by an automatic particle detector increases significantly during fog. Our research confirms that a large part of the fluorescent aerosol during fog is not pollen.

3. The fluorescence traces of airborne particles during fog have revealed that special conditions are formed, and this considerably enhances the number of organic particles in the air. Further research is needed to better understand the phenomenon. They are important because information needs to be integrated into bioaerosol particle identification systems working on an automatic regime.

ACKNOWLEDGEMENTS

This research has been supported by the European Social Fund (project no. 09.3.3-LMT-K-712-01-0066) under grant agreement with the Research Council of Lithuania (LMTLT). The authors are grateful to the Šiauliai Meteorological Station of the Lithuanian Hydrometeorological Service for providing meteorological data used in this research.

REFERENCES

Andreae M.O., Rosenfeld D. 2008. Aerosol–cloud–precipitation interactions. Part 1. The nature and sources of cloud-active aerosols. *Earth-Science Reviews,* 89: 13–41. https://doi.org/10.1016/j.earscirev.2008.03.001.

Auguie B., Antonov A., Auguie M.B. 2017. Package 'gridExtra'. https://cran.r-project.org/web/packages/gridExtra/gridExtra.pdf. Accessed date: 1 June 2020.

Avotniece Z., Klavins M., Lizuma L. 2015. Fog climatology in Latvia. *Theoretical and applied climatology,* 122: 97–109. https://doi.org/10.1007/s00704-014-1270-4.

Birdwell J.E., Valsaraj K.T. 2010. Characterization of dissolved organic matter in fogwater by excitation–emission matrix fluorescence spectroscopy. *Atmospheric Environment,* 44: 3246–3253. https://doi.org/10.1016/j.atmosenv.2010.05.055.

Biswas K.F., Ghauri B.M., Husain L. 2008. Gaseous and aerosol pollutants during fog and clear episodes in South Asian urban atmosphere. *Atmospheric Environment,* 42: 7775–7785. https://doi.org/10.1016/j.atmosenv.2008.04.056

Blackmore S., Wortley A.H., Skvarla J.J., Rowley J.R. 2007. Pollen wall development in flowering plants. *New Phytologist,* 174: 483–498. https://doi.org/10.1111/j.1469-8137.2007.02060.x.

Błaś M., Sobik M., Quiel F., Netzel P. 2002. Temporal and spatial variations of fog in the Western Sudety Mts., Poland. *Atmospheric Research*, 64: 19–28. https://doi.org/10.1016/S0169-8095(02)00076-5.

Chappuis C., Tummon F., Clot B., Konzelmann T., Calpini B., Crouzy B. 2020. Automatic pollen monitoring: first insights from hourly data. *Aerobiologia,* 36: 159–170. https://doi.org/10.1007/s10453-019-09619-6.

Clot B., Gilge S., Hajkova L., Magyar D., Scheifinger H., Sofiev M., ... Tummon F. 2020. The EUMETNET AutoPollen programme: establishing a prototype automatic pollen monitoring network in Europe. *Aerobiologia,* 1–9. https://doi.org/10.1007/s10453-020-09666-4

Croft P.J. 2003. Fog. In: Holton, J.A. Pyle, J.A. Curry (Eds.), Encyclopedia of Atmospheric Sciences, Academic Press, London, pp. 777–792.

Crouzy B., Stella M., Konzelmann T., Calpini B., Clot, B. 2016. All-optical automatic pollen identification: Towards an operational system. *Atmospheric Environment,* 140: 202–212. https://doi.org/10.1016/j.atmosenv.2016.05.062.

Daunys G., Šukienė L., Vaitkevičius L., Valiulis G., Sofiev M., Šaulienė I. 2021. Clustering approach for the analysis of the fluorescent bioaerosol collected by an automatic detector. Plos one 16: e0247284. https://doi.org/10.1371/journal.pone.0247284.

Després V., Huffman J.A., Burrows S. M., Hoose C., Safatov A., Buryak G., ... Jaenicke R. 2012. Primary biological aerosol particles in the atmosphere: a review. Tellus B: *Chemical and Physical Meteorology,* 64: 15598. https://doi.org/10.3402/tellusb.v64i0.15598.

Donaldson L. 2020. Autofluorescence in Plants. *Molecules,* 25: 2393. https://doi.org/10.3390/molecules25102393.

Dueker M.E., O'Mullan G.D., Weathers K.C., Juhl A. R., Uriarte M. 2012. Coupling of fog and marine microbial content in the near-shore coastal environment. *Biogeosciences,* 9: 803–813. https://doi.org/10.5194/bg-9-803-2012.

EEA, 2020 Air quality standards. Accessed July, 2020. https://www.eea.europa.eu/themes/air/air-quality-concentrations/air-quality-standards.

Environmental Protection Agency (EPA) (2020). 2019 m. oro kokybės duomenys (2019 air quality data). http://oras.gamta.lt/cms/index-?rubricId=5ab2efe4-a3b7-4387-9d26-3afd-8f514c51. Accessed on 30 of June, 2020. (In Lithuanian).

United States Environmental Protection Agency (USEPA) 2020. National ambient air quality standards. Accessed July, 2020. https://www.epa.gov/criteria-air-pollutants/naaqs-table.

Fröhlich-Nowoisky J., Kampf C.J., Weber B., Huffman J.A., Pöhlker C., Andreae M.O., ... Su H. 2016. Bioaerosols in the Earth system: Climate, health, and ecosystem interactions. *Atmospheric Research,* 182: 346–376. https://doi.org/10.1016/j.atmosres.2016.07.018.

Fu P., Kawamura K., Chen J., Qin M., Ren L., Sun Y., ... Yamashita Y. 2015. Fluorescent water-soluble organic aerosols in the High Arctic atmosphere. *Scientific reports,* 5: 9845. https://doi.org/10.1038/srep09845.

Fuzzi S., Mandrioli P., Perfetto A. 1997. Fog droplets - an atmospheric source of secondary biological aerosol particles. *Atmospheric environment,* 31: 287–290. https://doi.org/10.1016/1352-2310(96)00160-4.

Galvonaitė A., Valiukas D., Kilpys J., Kitrienė Z., Misiūnienė M. (2013). Lietuvos klimato atlasas. (Climate atlas of Lithuania). Lietuvos hidrometeorologijos tarnyba, 175 (In Lithuanian and in English).)

Goss K.U., 1994. Predicting the enrichment of organic compounds in fog caused by adsorption on the water surface. *Atmospheric Environment,* 28: 3513e3517. https://doi.org/10.1016/1352-2310(94)90008-6.

Grewling Ł., Nowak M., Szymańska A., Kostecki L., Bogawski P. 2019. Temporal variability in the allergenicity of airborne *Alternaria* spores. *Medical mycology,* 57: 403–411. https://doi.org/10.1093/mmy/myy069.

Heath A.A., Valsaraj K.T. 2017. An Experimental Study of the Atmospheric Oxidation of a Biogenic Organic Compound (Methyl Jasmonate) in a Thin Water Film as in Fog or Aerosols. *Open Journal of Air Pollution,* 6: 44. https://doi.org/10.4236/ojap.2017.62004.

Hůnová I., Brabec M., Malý M., Valeriánová A. 2018. Revisiting fog as an important constituent of the atmosphere. *Science of The Total Environment,* 636: 1490–1499. https://doi.org/10.1016/j.scitotenv.2018.04.322.

Hyde P., Mahalov A. 2020. Contribution of bioaerosols to airborne particulate matter. *Journal of the Air & Waste Management Association,* 70: 71–77. https://doi.org/10.1080/10962247.2019.1629360.

Jaenicke R. 2005. Abundance of cellular material and proteins in the atmosphere. *Science,* 308: 73–73. https://doi.org/10.1126/science.1106335

Kabir E., Azzouz A., Raza N., Bhardwaj S.K., Kim K.H., Tabatabaei M., Kukkar D. 2020. Recent Advances in Monitoring, Sampling, and Sensing Techniques for Bioaerosols in the Atmosphere. *ACS sensors,* 5: 1254–1267. https://doi.org/10.1021/acssensors.9b02585.

Kazil J., Stier, P., Zhang K., Quaas J., Kinne S., O'Donnell D., ... Feichter J. 2010. Aerosol nucleation and its role for clouds and Earth's radiative forcing in the aerosol-climate model ECHAM5-HAM. *Atmospheric Chemistry and Physics,* 10: 10733–10752. https://doi.org/10.5194/acp-10-10733-2010

Kerminen V.M., Lihavainen H., Komppula M., Viisanen Y., Kulmala M. 2005. Direct observational evidence linking atmospheric aerosol formation and cloud droplet activation. *Geophysical research letters,* 32: L14803. https://doi.org/10.1029/2005GL023130.

Kluska K., Piotrowicz K., Kasprzyk I. 2020. The impact of rainfall on the diurnal patterns of atmospheric pollen concentrations. *Agricultural and Forest Meteorology,* 291: 108042. https://doi.org/10.1016/j.agrformet.2020.108042

Lee H.J., Laskin A., Laskin J., Nizkorodov S.A. 2013. Excitation–emission spectra and fluorescence quantum yields for fresh and aged biogenic secondary organic aerosols. *Environmental science & technology,* 47: 5763–5770. https://doi.org/10.1021/es400644c.

Lewis E.R., Schwartz S. E. 2004. Sea salt aerosol production: mechanisms, methods, measurements, and models. *American geophysical union,* Volume 152.

Li F.S., Phyo P., Jacobowitz J., Hong M., Weng J.K. 2019. The molecular structure of plant sporopollenin. *Nature plants,* 5: 41–46. https://doi.org/10.1038/s41477-018-0330-7

Lim H.J., Carlton A.G., Turpin B.J. 2005. Isoprene forms secondary organic aerosol through cloud processing: Model simulations. *Environmental science & technology,* 39: 4441–4446. https://doi.org/10.1021/es048039h.

Lithuanian Hydrometeorological Service (LHMT) (2020). Klimato rajonavimas (Climate zoning). http://www.meteo.lt/klimato-rajonavimas. Accessed date: 30 June 2020. (In Lithuanian)

Maalick Z., Kühn T., Korhonen H., Kokkola H., Laaksonen A., Romakkaniemi S. 2016. Effect of aerosol concentration and absorbing aerosol on the radiation fog life cycle. *Atmospheric Environment,* 133: 26–33. https://doi.org/10.1016/j.atmosenv.2016.03.018.

Mainelis G. 2020. Bioaerosol sampling: Classical approaches, advances, and perspectives. *Aerosol Science and Technology,* 54: 496–519. https://doi.org/10.1080/02786826.2019.1671950.

Mazoyer M., Burnet F., Denjean C., Roberts G.C., Haeffelin M., Dupont J.C., Elias T. 2019. Experimental study of the aerosol impact on fog microphysics. *Atmospheric Chemistry and Physics,* 19: 4323–4344. https://doi.org/10.5194/acp-19-4323-2019.

Myszkowska D., Piotrowicz K., Ziemianin M., Bastl M., Berger U., Dahl Å., ... Czarnobilska E. 2021. Unusually high birch (*Betula* spp.) pollen concentrations in Poland in 2016 related to long-range transport (LRT) and the regional pollen occurrence. *Aerobiologia,* 37: 543–559. https://doi.org/10.1007/s10453-021-09703-w.

Pérez C. F., Gassmann M. I., Covi M. 2009. An evaluation of the airborne pollen–precipitation relationship with the superposed epoch method. *Aerobiologia,* 25: 313–320. https://doi.org/10.1007/s10453-009-9135-5.

Pöhlker C., Huffman J. A., Förster J. D., Pöschl U. 2013. Autofluorescence of atmospheric bioaerosols: spectral fingerprints and taxonomic trends of pollen. *Atmospheric Measurement Techniques,* 6: 3369–3392. https://doi.org/10.5194/amt-6-3369-2013.

R Core Team 2018. R: A Language and Environment for Statistical Computing. R Foundation for Statistical Computing. https://www.R-project.org/. Accessed date: 15 June 2020.

R Studio Team 2016. R Studio: Integrated Development for R. R Studio, Inc., Boston, MA URL. http://www.rstudio.com/. Accessed date: 1 June 2020.

Rathnayake C.M., Metwali N., Jayarathne T., Kettler J., Huang Y., Thorne P.S., ... Stone E.A. 2017. Influence of rain on the abundance of bioaerosols in fine and coarse particles. *Atmospheric Chemistry & Physics,* 17: 2459–2475. https://doi.org/10.5194/acp-17-2459-2017

Roshchina V.V., Melnikova E. V., Iashin V.A., Kamaukhov V.N. 2002. Autofluorescence of intact Equisetum arvense L. spores during their development. *Biofizika,* 47: 318–324.

Official Statistics Portal (OSP) 2019. Population and social statistics. https://osp.stat.gov.lt/pradinis. Accessed date: 5 March 2021.

Oteros J., Pusch G., Weichenmeier I., Heimann U., Möller R., Röseler S., ... Buters J. T. 2015. Automatic and online pollen monitoring. *International archives of allergy and immunology,* 167: 158–166. https://doi.org/10.1159/000436968

Šantl-Temkiv T., Sikoparija B., Maki T., Carotenuto F., Amato P., Yao M., ... DeMott P. J. 2020. Bioaerosol field measurements: Challenges and perspectives in outdoor studies. *Aerosol Science and Technology,* 54: 520–546. https://doi.org/10.1080/02786826.2019.1676395.

Šaulienė I., Šukienė L., Daunys G., Valiulis G., Lankauskas A., Kokina I., ... Gavarāne I. 2019a. Detection and microscopy of Alnus glutinosa pollen fluorescence peculiarities. *Forests,* 10: 959. https://doi.org/10.3390/f10110959.

Šaulienė I., Šukienė L., Daunys G., Valiulis G., Vaitkevičius L., Matavulj P., ... Crouzy B. 2019b. Automatic pollen recognition with the Rapid-E particle counter: the first-level procedure, experience and next steps. *Atmospheric Measurement Techniques,* 12: 3435–3452. https://doi.org/10.5194/amt-12-3435-2019.

Schumacher C.J., Pöhlker C., Aalto P., Hiltunen V., Petäjä T., Kulmala M., ... Huffman J.A. 2013. Seasonal cycles of fluorescent biological aerosol particles in boreal and semi-arid forests of Finland and Colorado. *Atmospheric Chemistry and Physics,* 13: 11987–12001. https://doi.org/10.5194/acp-13-11987-2013.

Shan Y., Liu X., Lin L., Ke Z., Lu Z. 2021. An improved representation of aerosol wet removal by deep convection and impacts on simulated aerosol vertical profiles. *Journal of Geophysical Research: Atmospheres,* 126: e2020JD034173. https://doi.org/10.1029/2020JD034173.

Shiraiwa M., Ueda K., Pozzer A., Lammel G., Kampf C. J., Fushimi A., … Sato K. 2017. Aerosol health effects from molecular to global scales. *Environmental Science & Technology,* 51: 13545–13567. https://doi.org/10.1021/acs.est.7b04417.

Siljamo P., Sofiev M., Severova E., Ranta H., Kukkonen J., Polevova S., ... Minin A. 2008. Sources, impact and exchange of early-spring birch pollen in the Moscow region and Finland. *Aerobiologia,* 24: 211–230. https://doi.org/10.1007/s10453-008-9100-8.

Stocker T.F., Qin D., Plattner G.K., Tignor M., Allen S.K., Boschung J., ... Midgley P.M. 2013. Climate change 2013: The physical science basis. Contribution of working group I to the fifth assessment report of the intergovernmental panel on climate change, 1535.

Sofiev M., Belmonte J., Gehrig R., Izquierdo R., Smith M., Dahl Å., Siljamo P. 2013. Airborne pollen transport. In: Sofiev M., Bergmann K-Ch. (eds.): Allergenic pollen, pp 127–159. Springer, Dordrecht. https://doi.org/10.1007/978-94-007-4881-1_5

Taylor P.E., Flagan R.C., Miguel A.G., Valenta R., Glovsky M.M. 2004. Birch pollen rupture and the release of aerosols of respirable allergens. *Clinical & Experimental Allergy,* 34: 1591–1596. https://doi.org/10.1111/j.1365-2222.2004.02078.x.

Urbanczyk J., Casado M.A. F., Díaz T.E., Heras P., Infante M., Borrego A. G. 2015. Spectral fluorescence variation of pollen and spores from recent peat-forming plants. *International journal of coal geology,* 131: 263–273. https://doi.org/10.1016/j.coal.2014.06.024.

Valentini S., Barnaba F., Bernardoni V., Calzolai G., Costabile F., Di Liberto L., ... Nava

S. 2020. Classifying aerosol particles through the combination of optical and physical-chemical properties: Results from a wintertime campaign in Rome (Italy). *Atmospheric Research,* 235: 104799. https://doi.org/10.1016/j.atmosres.2019.104799.

Warnes M.G.R., Bolker B., Bonebakker L., Gentleman R., Huber W. 2016. Package 'gplots'. Various R Programming Tools for Plotting Data. https://cran.r-project.org/web/packages/gplots/gplots.pdf. Accessed date: 1 June 2020.

Wickham H. 2016. ggplot2: Elegant Graphics for Data Analysis. Springer-Verlag New York. ISBN 978-3-319-24277-4, https://ggplot2.tidyverse.org, Accessed date: 1 June 2020.

Williams C.G., Després V. 2017. Northern Hemisphere forests at temperate and boreal latitudes are substantial pollen contributors to atmospheric bioaerosols. *Forest Ecology and Management,* 401: 187–191. https://doi.org/10.1016/j.foreco.2017.06.040.

World Meteorological Organization (WMO). 2019. Manual on Codes. International Codes, volume I., https://library.wmo.int/doc_num.php?explnum_id=10235.

Yan C., Sullivan A.P., Cheng Y., Zheng M., Zhang Y., Zhu T., Collett Jr.J.L. 2019. Characterization of saccharides and associated usage in determining biogenic and biomass burning aerosols in atmospheric fine particulate matter in the North China Plain. *Science of The Total Environment,* 650: 2939–2950. https://doi.org/10.1016/j.scitotenv.2018.09.325.

Zíková N., Pokorná P., Makeš O., Sedlák P., Pešice P., Ždímal V. 2020. Activation of atmospheric aerosols in fog and low clouds. *Atmospheric Environment,* 230: 117490. https://doi.org/10.1016/j.atmosenv.2020.117490.

Received: 14.04.2022.
Accepted: 19.04.2022.

SUPPLEMENT

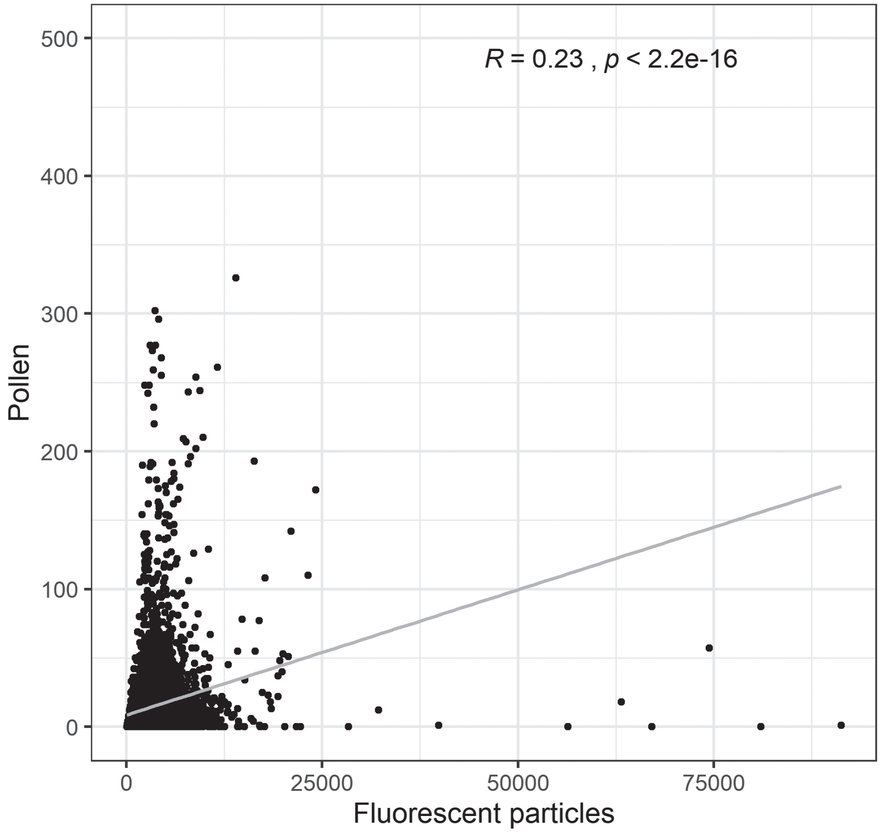

Figure 1. Distribution of identified airborne pollen in fluorescent aerosol.

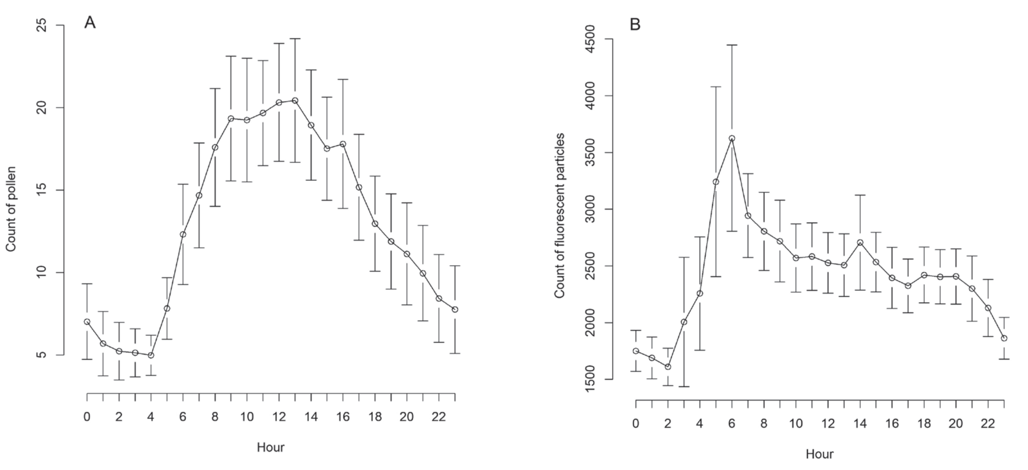

Figure 2. Daily distribution of particles detected by the automatic particle detector: A – the amount of identified pollen; B – the number of fluorescent particles (vertical lines – confidence interval).

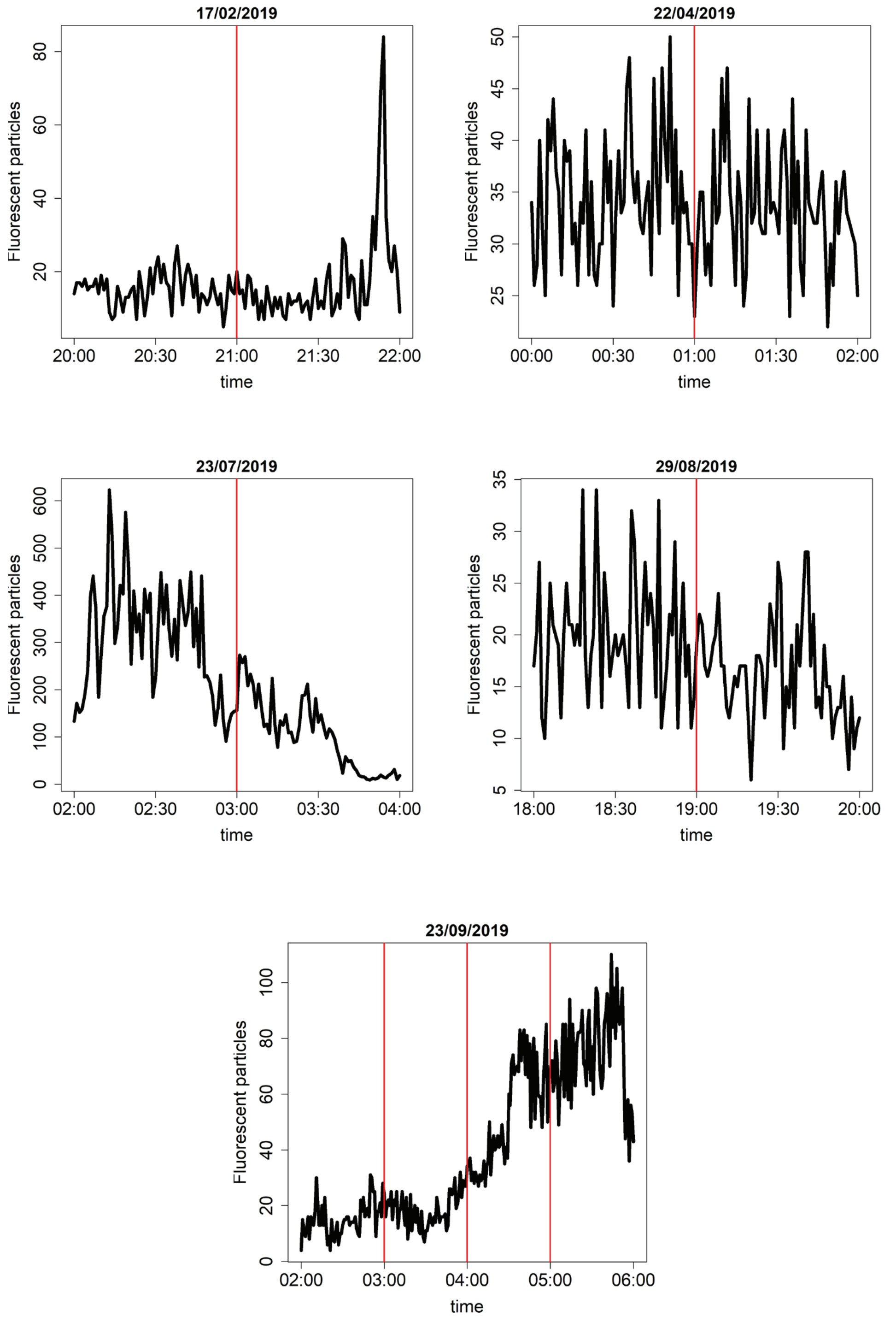

Figure 3. Numbers of particles making up fluorescent aerosol when fluorescence particles < 25 000 per hour and fog cases. The red line marks hours during which fog cases were recorded at the meteorological station (code: 41-47).